JAERI-M
8117

NEACRP-L-203

# EXPERIMENTAL STUDY OF LMFBR HETEROGENEOUS CORE AT FCA

March 1979

Masafumi NAKANO, Susumu IIJIMA, Keisho SHIRAKATA
and Jitsuya HIROTA

日本原子力研究所
Japan Atomic Energy Research Institute

# Experimental Study of LMFBR Heterogeneous Core at FCA

Masafumi NAKANO, Susumu IIJIMA[+], Keisho SHIRAKATA
and Jitsuya HIROTA

Division of Reactor Engineering, Tokai Research Establishment, JAERI

( Received January 30, 1979 )

In order to investigate physics properties of the heterogeneous LMFBR core and to examine reliability of the current data and method for heterogeneous core configuration, an experimental study has been made on FCA VII-3 Assembly which has an internal blanket ( IB ) at midplane of the cylindrical core. Systematic measurements of the criticality, sample worth, fission rate ratio, reaction rate distribution and sodium void worth were made on the heterogeneous cores whose IBs were different in composition and thickness.

The sodium void worth for the region from the midplane to the middle of the core decreases with increase of $^{238}U$ or Pu atomic density in IB. The worth is, however, not sensitive to composition of IB. The void worth in the core is lowered by about 35 % when the thickness of IB is increased from 20 cm to 40 cm.

The initial analysis using the JAERI-Fast Set Version II and the diffusion code CITATION was made for Assembly VII-3-1, the core with IB of 30 cm thickness. Comparison between the calculated and experimental results revealed the following : Pu worth is not well predicted in the core. Reaction rates sensitive to low energy neutrons are underestimated in IB when they are normalized in the core. A discontinuity of more than 20 % in the C/E value of the sodium void worth exists at the interface of IB and the core.

Keywords: LMFBR, Heterogeneous Core, Internal Blanket, FCA Assembly, Critical Experiment, Sodium Void Worth, Sample Worth, Reaction Rate Distribution

---

+) Division of Power Reactor Projects, JAERI

# ＦＣＡによる非均質高速炉心実験

日本原子力研究所東海研究所原子炉工学部
中野　正文・飯島　　進[†]
白方　敬章・弘田　実弥

（1979年1月30日受理）

非均質高速炉心の核特性評価に関する基礎研究としてFCA Ⅶ－3集合体により一連の実験を行った。実験体系は炉心中心に盤状の内部ブランケット（IB）を入れた単純形状の円筒炉心であり，IBの組成や厚みを変えて，臨界性，Naボイド効果，サンプル反応度価値，反応率分布等を系統的に測定した。IB中心から炉心中央までのNaボイド効果は，IB内の$^{238}$UおよびPu原子数密度の増加とともに減少する傾向が観測されたが，その変化はIBの組成にはあまり敏感ではない。IBの厚さが20 cmから40 cmに増すと炉心領域のNaボイド効果は約35％の減少を示した。

IB厚さ30 cmのFCA Ⅶ－3－1集合体について，JAERI－Fast Version Ⅱ，拡散近似による解析を行い測定値と比較した。計算値は低エネルギに感度の高い$^{235}$U（n，f），$^{238}$U（n，$\gamma$）等をIBで過少評価する。Puサンプル反応度価値の計算値は炉心領域の測定値をよく再現できない。NaボイドC効果のC／E値はIBと炉心の境界で20％以上の不連続性を示した。

†）動力炉開発・安全性研究管理部

Contents

# 目　　次

## 1. Introduction

From the viewpoints of lowering the sodium void worth and increasing the breeding gain in LMFBR, substaintial attention has been given to the heterogeneous core configuration. In order to investigate physics properties of the heterogeneous core and to examine reliability of the current data and method for heterogeneous core configuration, an experimental study has been made on FCA Assembly VII-3, which has an internal blanket at midplane of the cylindrical core.

Systematic measurements of the criticality, sodium void worth, sample worth, fission rate ratio and reaction rate distribution were made on the heterogeneous cores whose internal blankets were different in composition and thickness:

(i) about ±50 % variation of $^{238}U$ atomic density and addition of Pu fuel in the internal blanket, and

(ii) the internal blanket of 20 cm, 30 cm and 40 cm thickness.

Emphasis was placed on the measurement of axial distributions of sodium void worth, sample worth and reaction rate in the central region of the internal blanket and the core, since the axial heterogeneous configuration was limited to the central test region of the assembly, which was surrounded radially by the driver and the blanket regions.

In the present paper, experimental results are given of the effects of internal blanket composition and thickness. The calculated results with the JAERI-Fast Set Version-II with 25-group structure(1) and the diffusion theory are given in comparison with the experiments for Assembly VII-3-1, the core with the internal blanket of 30 cm thickness. Discussion is also made briefly of the results for each measurement.

## 2. Experimental procedure

Experiment was first made on FCA Assembly VII-3-1, which had a fertile zone of 30 cm thickness at midplane of the cylindrical core. R-Z configuration of Assembly VII-3-1 is shown in Fig. 1. The internal blanket is inserted in the central test region, about 70 cm in diameter. The core, about 90 cm in total height, is followed by the axial blanket 35 cm thick. Figure 2 illustrates plate arrangement of the test region drawer of Assembly VII-3-1. The Pu plates in the core were replaced by natural uranium metal and stainless steel plates in the internal and axial blankets. The average

## 1. Introduction

From the viewpoints of lowering the sodium void worth and increasing the breeding gain in LMFBR, substaintial attention has been given to the heterogeneous core configuration. In order to investigate physics properties of the heterogeneous core and to examine reliability of the current data and method for heterogeneous core configuration, an experimental study has been made on FCA Assembly VII-3, which has an internal blanket at midplane of the cylindrical core.

Systematic measurements of the criticality, sodium void worth, sample worth, fission rate ratio and reaction rate distribution were made on the heterogeneous cores whose internal blankets were different in composition and thickness:

(i) about ±50 % variation of $^{238}U$ atomic density and addition of Pu fuel in the internal blanket, and

(ii) the internal blanket of 20 cm, 30 cm and 40 cm thickness.

Emphasis was placed on the measurement of axial distributions of sodium void worth, sample worth and reaction rate in the central region of the internal blanket and the core, since the axial heterogeneous configuration was limited to the central test region of the assembly, which was surrounded radially by the driver and the blanket regions.

In the present paper, experimental results are given of the effects of internal blanket composition and thickness. The calculated results with the JAERI-Fast Set Version-II with 25-group structure(1) and the diffusion theory are given in comparison with the experiments for Assembly VII-3-1, the core with the internal blanket of 30 cm thickness. Discussion is also made briefly of the results for each measurement.

## 2. Experimental procedure

Experiment was first made on FCA Assembly VII-3-1, which had a fertile zone of 30 cm thickness at midplane of the cylindrical core. R-Z configuration of Assembly VII-3-1 is shown in Fig. 1. The internal blanket is inserted in the central test region, about 70 cm in diameter. The core, about 90 cm in total height, is followed by the axial blanket 35 cm thick. Figure 2 illustrates plate arrangement of the test region drawer of Assembly VII-3-1. The Pu plates in the core were replaced by natural uranium metal and stainless steel plates in the internal and axial blankets. The average composition smeared over the internal blanket and core is similar to the inner core composition of the prototype fast breeder reactor. The test region is surrounded radially by the driver of Pu and/or $^{235}U$ fuel. The composition of the driver was closely matched to that of the test region core. Assembly VII-3-1 is, therefore, considered as a single core system in which a fertile zone of 30 cm thickness is inserted.

Axial distribution of fission and capture rates were measured in the center drawer of the assembly. Measurements of fission rates for $^{239}Pu$, $^{235}U$, $^{238}U$ and $^{237}Np$ were made by traversing the micro fission counters of Pu, enriched U, depleted U and Np (6 mm-diameter and 32 mm or 35 mm-effective length) in the axial experimental hole made at the position of the $Al_2O_3$ and Na plates in the cell (see Fig. 2). Capture reaction rates for $^{238}U$ were measured by irradiating depleted U foils (12.7 mm-diameter and 0.025 mm-thickness) placed between the $Al_2O_3$ and depleted $UO_2$ plates.

Figure 3 shows 9 drawers around the axis of the assembly, used for the measurement of axial distribution of sodium void worth. Each region of 3×3×1 packs in the central 9 drawer was individually voided, where the pack means the unit size of FCA Assembly, i.e. a cuboid of $5.52 \times 5.52 \times 5.08$ $cm^3$. Channel void worth was also measured using the 9 drawers in the fixed half of FCA Assembly.

Axial sample worth distributions of Pu and depleted $UO_2$ were measured using the 4 drawers adjacent to the center drawer. The samples used are the standard plates same as those loaded in the core cell. Four plates were used for the measurement of Pu worth, and eight plates for the measurement of depleted $UO_2$ worth.

Reactivity change was determined from calibrated control rod positions. The reactivity scale based on the positive period measurement was converted to the absolute unit of $\Delta k/k$ using the delayed neutron data evaluated by Tomlinson(2). The measured worths were corrected for the drift of the core temperature (usually 0.1°C ∿ 0.3°C). The experimental error in the measurement of small reactivity change was estimated to be $\pm 1 \sim 2 \times 10^{-6}$ $\Delta k/k$, in which the uncertainty of the kinetic parameters used in the control rod calibration is not included.

## 3. Effects of internal blanket composition

The effects of internal blanket composition were studied on Assembly VII-3-1 by modifying the composition of the internal blanket 30 cm thick.

composition smeared over the internal blanket and core is similar to the inner core composition of the prototype fast breeder reactor. The test region is surrounded radially by the driver of Pu and/or $^{235}U$ fuel. The composition of the driver was closely matched to that of the test region core. Assembly VII-3-1 is, therefore, considered as a single core system in which a fertile zone of 30 cm thickness is inserted.

Axial distribution of fission and capture rates were measured in the center drawer of the assembly. Measurements of fission rates for $^{239}Pu$, $^{235}U$, $^{238}U$ and $^{237}Np$ were made by traversing the micro fission counters of Pu, enriched U, depleted U and Np (6 mm-diameter and 32 mm or 35 mm-effective length) in the axial experimental hole made at the position of the $Al_2O_3$ and Na plates in the cell (see Fig. 2). Capture reaction rates for $^{238}U$ were measured by irradiating depleted U foils (12.7 mm-diameter and 0.025 mm-thickness) placed between the $Al_2O_3$ and depleted $UO_2$ plates.

Figure 3 shows 9 drawers around the axis of the assembly, used for the measurement of axial distribution of sodium void worth. Each region of 3×3×1 packs in the central 9 drawer was individually voided, where the pack means the unit size of FCA Assembly, i.e. a cuboid of 5.52 × 5.52 × 5.08 $cm^3$. Channel void worth was also measured using the 9 drawers in the fixed half of FCA Assembly.

Axial sample worth distributions of Pu and depleted $UO_2$ were measured using the 4 drawers adjacent to the center drawer. The samples used are the standard plates same as those loaded in the core cell. Four plates were used for the measurement of Pu worth, and eight plates for the measurement of depleted $UO_2$ worth.

Reactivity change was determined from calibrated control rod positions. The reactivity scale based on the positive period measurement was converted to the absolute unit of $\Delta k/k$ using the delayed neutron data evaluated by Tomlinson(2). The measured worths were corrected for the drift of the core temperature (usually 0.1°C ∿ 0.3°C). The experimental error in the measurement of small reactivity change was estimated to be $\pm 1 \sim 2 \times 10^{-6}$ $\Delta k/k$, in which the uncertainty of the kinetic parameters used in the control rod calibration is not included.

## 3. Effects of internal blanket composition

The effects of internal blanket composition were studied on Assembly VII-3-1 by modifying the composition of the internal blanket 30 cm thick.

Two depleted $UO_2$ plates in the internal blanket cell were replaced by stainless steel plates for reduction of $^{238}U$ atomic density (SUS IB), while they were replaced by natural uranium metal plates for increase of $^{238}U$ (NU IB). The change of $^{238}U$ atomic density thus modified is -49 % for the SUS IB and +56 % for the NU IB. Simulation of Pu build-up in the internal blanket was made by replacing half the SUS plate by the corresponding half Pu plate in each cell (Pu IB). The Pu atomic density added in the internal blanket is about 16 % of that in the core.

The change of criticality was compensated by adjusting the driver thickness, the diameter of the central test region being fixed. To minimize the change of critical mass, however, modification of the internal blanket composition was limited to the central zone, about 42 cm in diameter. As far as the physics properties along the axis are concerned, no significant effect of keeping the outer zone of the internal blanket as the reference composition was expected by calculation. The deviation of the driver volume from the reference core was -2 % in the SUS IB, +1 % in the NU IB and -4 % in the Pu IB.

The axial distributions of $^{239}Pu$ and $^{238}U$ fission rates normalized in the outer half of the core region are shown in Figs. 4 and 5, respectively. In the reference core, the $^{239}Pu$ fission rate slightly increases from the middle of the core to the center of the internal blanket, but it decreases in the internal blanket of the NU IB. On the other hand, remarkable increase of the $^{239}Pu$ fission rate is observed in the internal blanket of the SUS IB. At the center of the internal blanket, the change of the fission rate from the reference core is about +20 % in the SUS IB and about -20 % in the NU IB. $^{239}Pu$ fission rate distribution of the PU IB is nearly flat in the internal blanket and the inner half of the core. The fission rate of $^{238}U$ goes down steeply towards the internal blanket. Compared with the reference core, the $^{238}U$ fission rate in the internal blanket is slightly decreased in both the SUS IB and the NU IB, but in the Pu IB it is remarkably increased due to the increase of fission source.

The axial distributions of Pu and deplated $UO_2$ worths are shown in Fig. 6. The distribution of Pu worth is different from that of the $^{239}Pu$ fission rate. The Pu worth in the reference core, for example, becomes a maximum in the core and decreases in the internal blanket. As seen in the figure, the Pu worths measured in the middle of the core are almost same within ±5 % in the cores studied. In the internal blanket, the Pu worth decreases with increase of the $^{238}U$ atomic density in the internal blanket. However, the change of the relative value of Pu worth normalized in the middle of the core is smaller than that of the $^{239}Pu$ fission rate. This indicates that the fission neutron importance in the internal blanket increases with increase of the $^{238}U$ atomic density in the internal blanket when the importance is normalized in the middle of the core. The axial distribution of depleted $UO_2$ worth in the internal blanket and the inner half of the core is similar to that of the Pu worth.

Figure 7 shows the axial distributions of sodium void worth measured using the central 9 drawers. There is a valley at the interface of the internal blanket and the core, and the void worth at the center of the internal blanket is more positive than that in the core. An increase of about 10 % of the void worth is observed at the center of the internal blanket of the SUS IB. The void worth is lowered by about 5 % at the center of the internal blanket and by about 10 % near the interface in the case of the NU IB. In the Pu IB, a slight reduction of the void worth is observed in both the internal blanket and the inner half of the core.

The worths of simultaneous voiding from the center of the internal blanket to the middle of the core were also compared. The void worth was increased by about 7 % in the SUS IB, while it was lowered by about 8 % in the NU IB and by about 5 % in the Pu IB. Therefore, it can be concluded that the sodium void worth is not sensitive to composition of the internal blanket.

## 4. Effects of internal blanket thickness

The effects of internal blanket thickness were investigated on the assemblies with the internal blanket of 20 cm, 30 cm and 40 cm thickness. The total height of the core and Pu content in the core are fixed for the three assemblies. The atomic density of Pu in the core is, therefore, increased with increase of the internal blanket thickness. The internal blanket of the reference composition is commonly used for the three assemblies. The change of criticality was compensated by adjusting the driver thickness. The driver volume was reduced by about 2 % in the 20 cm IB and increased by about 7 % in the 40 cm IB, compared with that of the 30 cm IB.

The axial fission rate distributions for $^{239}Pu$ and $^{238}U$ are shown in Figs. 8 and 9, respectively. The $^{239}Pu$ fission rate increases in the decreases with increase of the $^{238}U$ atomic density in the internal blanket. However, the change of the relative value of Pu worth normalized in the middle of the core is smaller than that of the $^{239}Pu$ fission rate. This indicates that the fission neutron importance in the internal blanket increases with increase of the $^{238}U$ atomic density in the internal blanket when the importance is normalized in the middle of the core. The axial distribution of depleted $UO_2$ worth in the internal blanket and the inner half of the core is similar to that of the Pu worth.

Figure 7 shows the axial distributions of sodium void worth measured using the central 9 drawers. There is a valley at the interface of the internal blanket and the core, and the void worth at the center of the internal blanket is more positive than that in the core. An increase of about 10 % of the void worth is observed at the center of the internal blanket of the SUS IB. The void worth is lowered by about 5 % at the center of the internal blanket and by about 10 % near the interface in the case of the NU IB. In the Pu IB, a slight reduction of the void worth is observed in both the internal blanket and the inner half of the core.

The worths of simultaneous voiding from the center of the internal blanket to the middle of the core were also compared. The void worth was increased by about 7 % in the SUS IB, while it was lowered by about 8 % in the NU IB and by about 5 % in the Pu IB. Therefore, it can be concluded that the sodium void worth is not sensitive to composition of the internal blanket.

## 4. Effects of internal blanket thickness

The effects of internal blanket thickness were investigated on the assemblies with the internal blanket of 20 cm, 30 cm and 40 cm thickness. The total height of the core and Pu content in the core are fixed for the three assemblies. The atomic density of Pu in the core is, therefore, increased with increase of the internal blanket thickness. The internal blanket of the reference composition is commonly used for the three assemblies. The change of criticality was compensated by adjusting the driver thickness. The driver volume was reduced by about 2 % in the 20 cm IB and increased by about 7 % in the 40 cm IB, compared with that of the 30 cm IB.

The axial fission rate distributions for $^{239}Pu$ and $^{238}U$ are shown in Figs. 8 and 9, respectively. The $^{239}Pu$ fission rate increases in the internal blanket in each assembly. The distribution, however, becomes more flat by increasing the internal blanket thickness. As shown in Fig. 9, the maximum fission rate of $^{238}U$ was obtained at a point in the core, about 13 cm from the internal blanket-core boundary, in each assembly. The $^{238}U$ fission rate at the center of the internal blanket decreases with increase of the internal blanket thickness when the peak value of each assembly is normalized to unity. The value at the center of the 40 cm IB is nearly half that of the 20 cm IB.

The axial distributions of Pu sample worth are compared in Fig. 10. The distribution in the 20 cm IB is nearly flat in the internal blanket and the inner part of the core, while remarkable decrease of the Pu worth is observed in the internal blanket in the case of the 40 cm IB. The value at the center of the internal blanket is decreased by about 8 % in the case of the 30 cm IB and by about 25 % in the 40 cm IB, compared with that in the 20 cm IB.

Figure 11 shows the axial distributions of sodium void worth measured in the three assemblies. The valley at the internal blanket-core boundary is not clear in the case of the 20 cm IB, but it is very deep in the 40 cm IB. The void worth at the boundary decreases with increase of the internal blanket thickness. The void worths in the internal blanket and the core and the channel void worth in each assembly are given in Table 1. The channel void worth is not sensitive to thickness of the internal blanket, although it tends to decrease with increase of the internal blanket thickness. The void worth in the internal blanket increases with increase of the thickness. The average value per unit volume is, however, considerably lowered by increasing the thickness. The void worth in the core lowers with increase of the internal blanket thickness. The reduction observed is about 35 % from the 20 cm IB to the 40 cm IB.

## 5. Comparison of calculation with experiment

Calculations for Assembly VII-3-1 were made using the JAERI-Fast Set Version II with 25-group structure. R-Z diffusion calculation was made with the CITATION code(3), using the cell averaged 25-group cross sections prepared by the collision probability method. The directional diffusion coefficients based on the Benoist's formula(4) were used in the calculation. The C/E value of 0.998 was obtained for the criticality, where the transport correction of 0.8 $\%\Delta k/k$ is included.

internal blanket in each assembly. The distribution, however, becomes more flat by increasing the internal blanket thickness. As shown in Fig. 9, the maximum fission rate of $^{238}U$ was obtained at a point in the core, about 13 cm from the internal blanket-core boundary, in each assembly. The $^{238}U$ fission rate at the center of the internal blanket decreases with increase of the internal blanket thickness when the peak value of each assembly is normalized to unity. The value at the center of the 40 cm IB is nearly half that of the 20 cm IB.

The axial distributions of Pu sample worth are compared in Fig. 10. The distribution in the 20 cm IB is nearly flat in the internal blanket and the inner part of the core, while remarkable decrease of the Pu worth is observed in the internal blanket in the case of the 40 cm IB. The value at the center of the internal blanket is decreased by about 8 % in the case of the 30 cm IB and by about 25 % in the 40 cm IB, compared with that in the 20 cm IB.

Figure 11 shows the axial distributions of sodium void worth measured in the three assemblies. The valley at the internal blanket-core boundary is not clear in the case of the 20 cm IB, but it is very deep in the 40 cm IB. The void worth at the boundary decreases with increase of the internal blanket thickness. The void worths in the internal blanket and the core and the channel void worth in each assembly are given in Table 1. The channel void worth is not sensitive to thickness of the internal blanket, although it tends to decrease with increase of the internal blanket thickness. The void worth in the internal blanket increases with increase of the thickness. The average value per unit volume is, however, considerably lowered by increasing the thickness. The void worth in the core lowers with increase of the internal blanket thickness. The reduction observed is about 35 % from the 20 cm IB to the 40 cm IB.

## 5. Comparison of calculation with experiment

Calculations for Assembly VII-3-1 were made using the JAERI-Fast Set Version II with 25-group structure. R-Z diffusion calculation was made with the CITATION code[3], using the cell averaged 25-group cross sections prepared by the collision probability method. The directional diffusion coefficients based on the Benoist's formula[4] were used in the calculation. The C/E value of 0.998 was obtained for the criticality, where the transport correction of 0.8 %Δk/k is included.

The reaction rates along the axis were calculated using the cell averaged reaction cross sections in each cell. The C/E values of the reaction rate distributions are summarized in Table 2, where the calculated values are normalized to the experiments at the position of core Z = 27.9 cm. Agreement is good between the calculated and the experimental fission rates for $^{239}Pu$. The calculation, however, tends to overstimate the $^{238}U$ fission rate and to underestimate the $^{235}U$ fission and $^{238}U$ capture rates in the internal blanket.

The axial distributions of the sample worths and the sodium void worth of 3 × 3 × 1 packs voiding were calculated by first order perturbation approximation. To deal with the plate heterogeneity in the cells, the cell averaged cross sections were prepared for both the perturbed and the unperturbed cells. The calculated values of Pu and depleted $UO_2$ worths are compared with the experiments in Table 3. Agreement is good between the calculated and the experimental Pu worth in the internal blanket. The calculation, however, considerably underestimates the experiment in the core. For the depleted $UO_2$ worth, the calculation considerably underestimates the experiment in the internal blanket and the inner half of the core.

The calculated sodium void worths are compared with the experimental ones in Table 4. The calculated values for the simultaneous voidings of 13 ∿ 16Z (the outer region of the axial blanket) and of 1 ∿ 16Z (the channel void) were obtained with the exact perturbation theory. The calculation predicts the experiment fairly well for the channel void worth as well as for the axial distribution of the sodium void worth. However, a discontinuity of more than 20 % in the C/E value is observed at the interface of the internal blanket and the core: The calculation overestimates the experiment by about 10% the internal blanket,and it understimates by more than 10 % in the core.

The axial distribution of the calculated void worth is shown in Fig. 12, together with the leakage and non-leakage components. It is seen that the valley in the void worth distribution coincides with the variation of the leakage component which becomes a maximum near the internal blanket-core boundary. The distribution of non-leakage component, about 80 % of which is the moderation term, is nearly flat in the internal blanket, but the value decreases to about 2/3 at inner edge of the core. It is thus indicated that the discontinuity of the C/E values at the interface is mainly caused by poor prediction of the moderation term by the 25-group calculation.

## 6. Conclusion

An experimental study has been made on FCA Assembly VII-3, which has an internal blanket at midplane of the cylindrical core. Emphasis was placed on the measurement of axial distributions of sodium void worth, sample worth and reaction rate in the central region of the internal blanket and the core.

In the axial distribution of sodium void worth, there is a valley at the internal blanket-core boundary, and the void worth at the center of the internal blanket is more positive than that in the core. The valley in the void worth distribution coincides with the variation of the leakage component which becomes a maximum near the boundary.

The sodium void worth for the region from the midplane to the middle of the core decreases with increase of $^{238}U$ or Pu atomic density in the internal blanket. The worth is, however, not sensitive to composition of the internal blanket. One of the causes is probably the competition between the variations of the importance spectrum and the flux level in the internal blanket.

The void worth in the internal blanket increases with increase of the internal blanket thickness. On the other hand, the void worth in the core is decreases with increase of the thickness. The reduction observed is about 35 % from the 20 cm IB to the 40 cm IB. The channel void worth is not sensitive to the thickness of the internal blanket, although it tends to decrease with increase of the internal blanket thickness.

The calculated results with the JAERI-Fast Set Version II and the diffusion theory were compared with the experiment for Assembly VII-3-1. Agreement is good between the calculation and the experiment for the $^{239}Pu$ fission rate distribution. However, the Pu sample worth is not well predicted in the core. The calculation overestimates the $^{238}U$ fission rate and underestimates the $^{238}U$ capture rate in the internal blanket when normalized to the experiment in the core. These tendencies are similar to those observed in the radial blanket.

The calculation predicts the experiment fairly well for the channel void worth as well as for the axial distribution of sodium void worth. However, a discontinuity of more than 20 % in the C/E value is observed at the interface of internal blanket and core. This may be caused by poor prediction of the moderation term by the 25-group calculation.

## Acknowledgement

The authors wish to express their thanks to Mr. A. Hasegawa (now in OECD NEA Data Bank), who contributed to the planning and to the early work of the experiment. They thank also to FCA staff for their support in the experiment.

## References

(1) Takano, H., et al.: JAERI Fast Reactor Group Constants Set, Version II, JAERI 1255 (1978).

(2) Tomlinson, L.: Delayed Neutrons from Fission, AERE-R 6993 (1972).

(3) Fowler, T., et al.: Nuclear Reactor Core Analysis Code: CITATION, ORNL-TM-2496 (1969).

(4) Benoist, P.: A General Formulation of the Diffusion Coefficient in a Heterogeneous Medium Which May Contain Cavity, AERE-Trans. 842 (1959).

Acknowledgement

The authors wish to express their thanks to Mr. A. Hasegawa (now in OECD NEA Data Bank), who contributed to the planning and to the early work of the experiment. They thank also to FCA staff for their support in the experiment.

References

(1) Takano, H., et al.: JAERI Fast Reactor Group Constants Set, Version II, JAERI 1255 (1978).

(2) Tomlinson, L.: Delayed Neutrons from Fission, AERE-R 6993 (1972).

(3) Fowler, T., et al.: Nuclear Reactor Core Analysis Code: CITATION, ORNL-TM-2496 (1969).

(4) Benoist, P.: A General Formulation of the Diffusion Coefficient in a Heterogeneous Medium Which May Contain Cavity, AERE-Trans. 842 (1959).

Table 1 Sodium void worth measured in the central 3×3 drawers of FCA Assembly VII-3

($\times 10^{-6}$ Δk/k)

| Assembly | I.B. | Core | Channel void |
|---|---|---|---|
| 20 cm IB | 120 | 108* | 122 |
| 30 cm IB | 153 | 81 | 115 |
| 40 cm IB | 168* | 70* | 104 |

* : indirect measurement

Table 2 C/E values for axial reaction rate distribution of FCA Assembly VII-3-1

| Region | Distance from midplane Z (cm) | C/E | | | |
|---|---|---|---|---|---|
| | | $^{239}$Pu(n,f) | $^{235}$U(n,f) | $^{238}$U(n,f) | $^{238}$U(n,γ) |
| Internal blanket | 2.5 | 1.01 | 0.97 | 1.08 | 0.90 |
| | 7.6 | 1.01 | 0.97 | 1.13 | 0.92 |
| | 12.7 | 1.02 | 0.98 | 1.14 | 0.92 |
| Core | 15.2 | 0.99 | 0.99 | 1.07 | 0.96 |
| | 17.8 | 0.98 | 1.00 | 0.99 | 1.00 |
| | 22.9 | 1.00 | 1.01 | 0.99 | 1.01 |
| | 27.9 | 1.00 | 1.00 | 1.00 | 1.00 |
| | 33.0 | 1.01 | 1.00 | 1.00 | 0.97 |
| | 38.1 | 0.99 | 1.00 | 0.98 | - |
| | 43.2 | 0.98 | 0.99 | 0.97 | 1.00 |
| Axial blanket | 45.7 | 0.98 | - | 1.01 | 0.97 |
| | 48.3 | 1.00 | 0.97 | 1.09 | 0.91 |
| | 53.3 | 0.98 | 0.94 | 1.11 | - |
| | 58.4 | 0.96 | 0.92 | 1.06 | 0.84 |

Note: Calculated values are normalized to the experiments at Z = 27.9 cm.

Table 3 Comparison of experimental and calculated sample worths along the axis of FCA Assembly VII-3-1

| Region | Position | Pu sample | | | Depleted $UO_2$ sample | | |
|---|---|---|---|---|---|---|---|
| | | Experiment ($10^{-4}\Delta k/k$) | Calculated ($10^{-4}\Delta k/k$) | C/E | Experiment ($10^{-4}\Delta k/k$) | Calculated ($10^{-4}\Delta k/k$) | C/E |
| Internal blanket | 1Z | 2.37±0.02 | 2.35 | 0.99 | -1.14±0.02 | -1.07 | 0.94 |
| | 2Z | 2.40±0.02 | 2.36 | 0.98 | | | |
| | 3Z | 2.43±0.02 | 2.38 | 0.98 | -1.15±0.02 | -0.98 | 0.87 |
| Core | 4Z | 2.54±0.02 | 2.33 | 0.92 | -1.20±0.02 | -1.04 | 0.86 |
| | 5Z | 2.62±0.02 | 2.40 | 0.92 | -1.26±0.02 | -1.13 | 0.89 |
| | 6Z | 2.54±0.02 | 2.33 | 0.92 | -1.13±0.02 | -1.02 | 0.90 |
| | 7Z | 2.27±0.02 | 2.09 | 0.92 | | | |
| | 9Z | 1.43±0.02 | 1.29 | 0.90 | -0.04±0.02 | +0.22 | |
| Axial blanket | 10Z | 1.02±0.02 | 0.94 | 0.92 | +0.20±0.02 | +0.35 | |
| | 12Z | 0.424±0.01 | 0.379 | 0.89 | +0.30±0.02 | +0.13 | |

Table 4 Comparison of experimental and calculated sodium void worths for the central 3×3 drawers of FCA Assembly VII-3-1

| Region voided (cell unit) | Experiment ($10^{-6}\Delta k/k$) | Calculation ($10^{-6}\Delta k/k$) | C-E ($10^{-6}\Delta k/k$) | $\frac{C-E}{\lvert E \rvert}$ (%) |
|---|---|---|---|---|
| 1Z | 64.4±1.4 | 69.0 | +4.6 | +7 |
| 2Z | 54.9±1.1 | 62.4 | +7.5 | +14 |
| 3Z | 44.1±1.1 | 50.8 | +6.7 | +15 |
| 4Z | 39.7±1.1 | 35.3 | -4.4 | -11 |
| 5Z | 45.9±1.1 | 40.2 | -5.7 | -12 |
| 6Z | 37.9±1.1 | 34.4 | -3.5 | -9 |
| 7Z | 18.6±1.2 | 14.5 | -4.1 | -22 |
| 8Z | -14.6±1.0 | -15.4 | -0.8 | -15 |
| 9Z | -43.1±1.0 | -47.3 | -4.2 | -10 |
| 10Z | -48.4±1.1 | -49.4 | -1.0 | -2 |
| 11Z | -30.7±1.0 | -30.3 | +0.4 | +1 |
| 12Z | -18.9±1.1 | -17.5 | +1.4 | +7 |
| 13∿16Z | -21.5±1.1 | -25.0 | -3.5 | -16 |
| 1∿16Z | 114.8±1.2 | 141 | +26 | +23 |

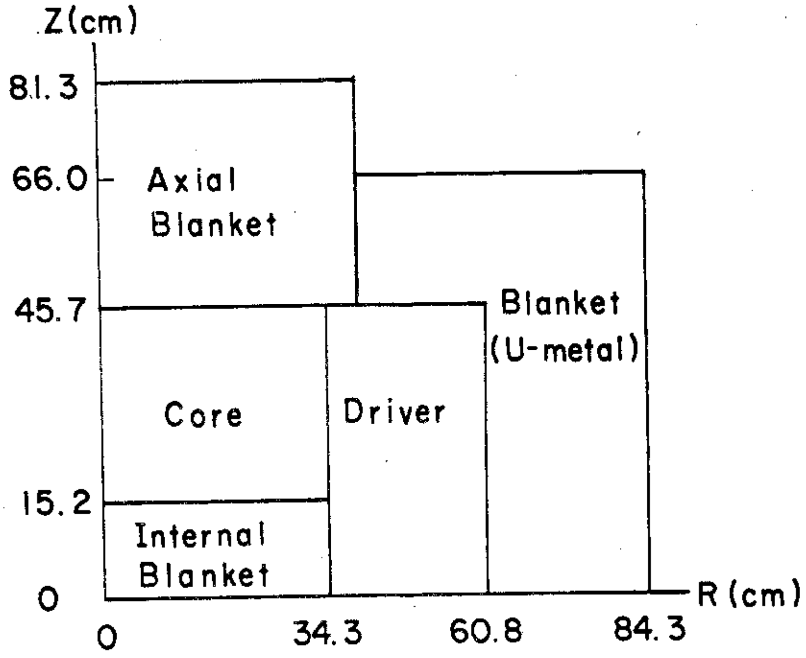


Fig. 1 R-Z configuration of
FCA Assembly VII-3-1.

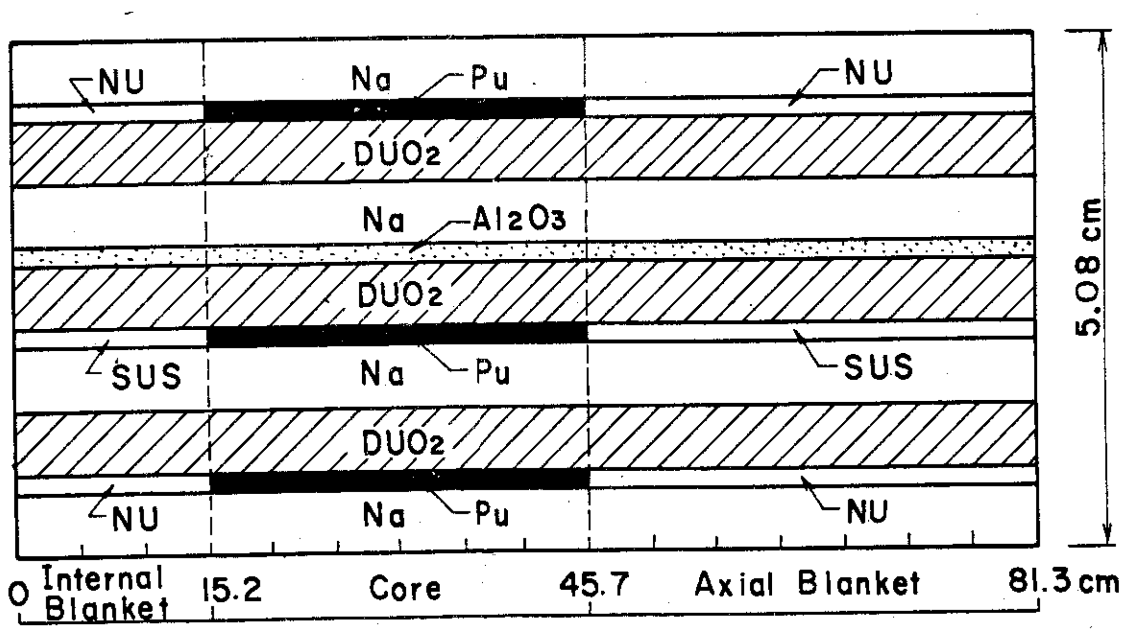


Fig. 2 Loading Pattern of test zone drawer of FCA Assembly VII-3-1.

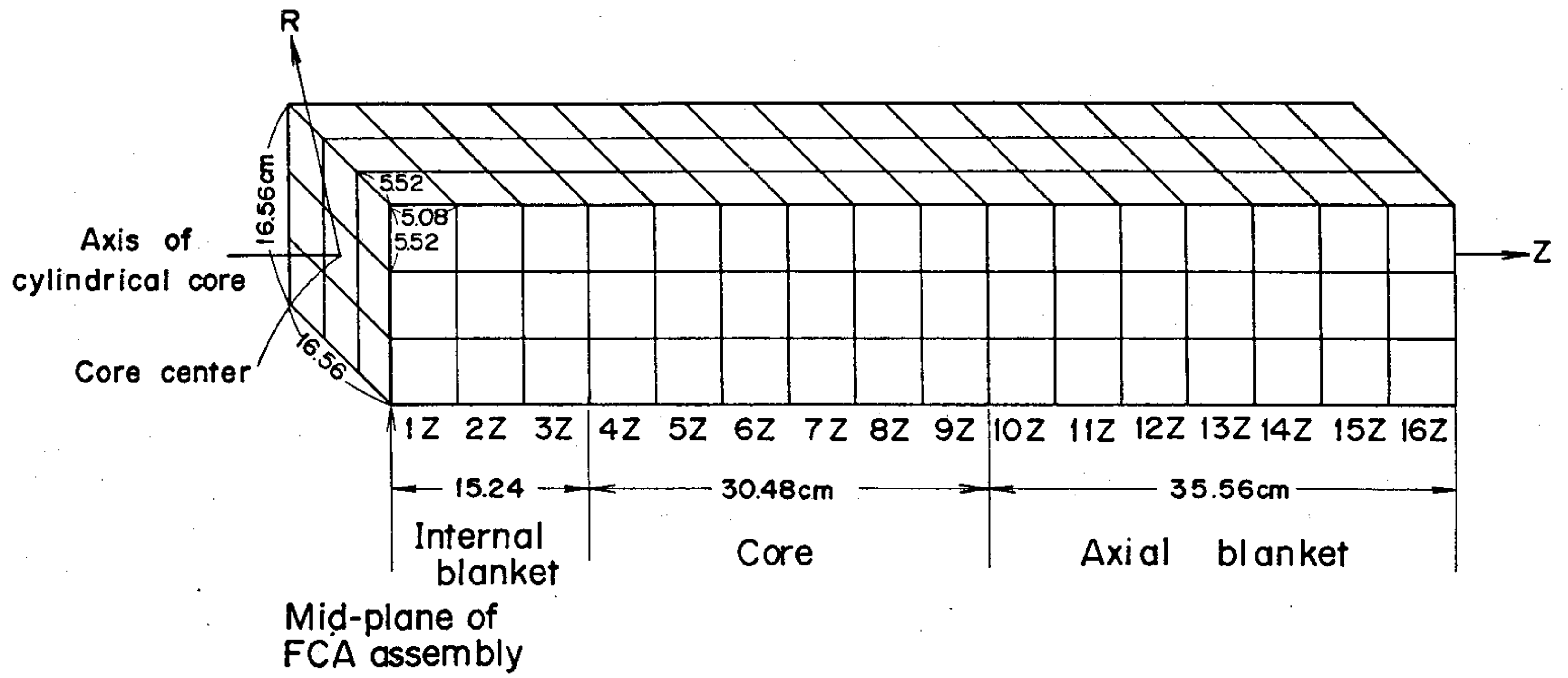


Fig. 3 The 9 drawers around the axis of FCA Assembly VII-3-1 used for measurement of axial distribution of sodium void worth.

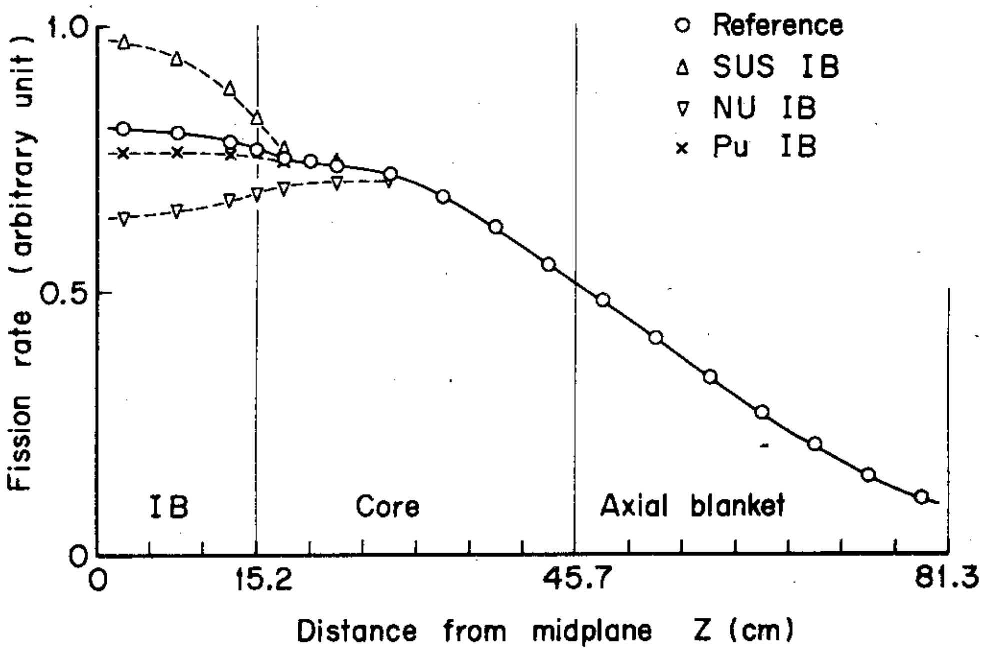


Fig. 4 Axial fission rate distributions of Pu-239 mfc measured in FCA Assembly VII-3-1.

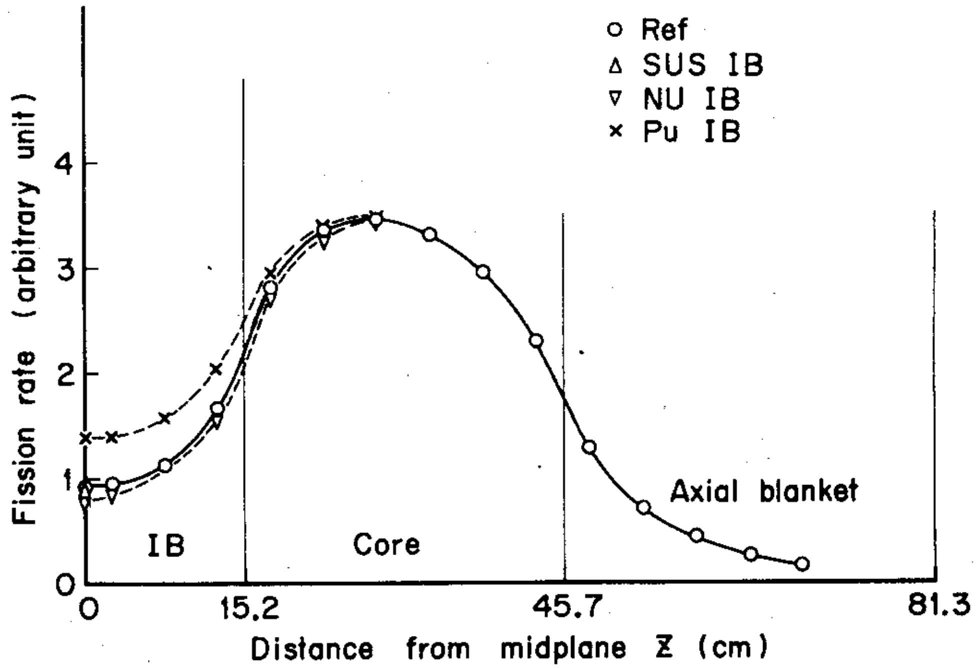


Fig. 5 Axial fission rate distributions of depleted U mfc measured in FCA Assembly VII-3-1.

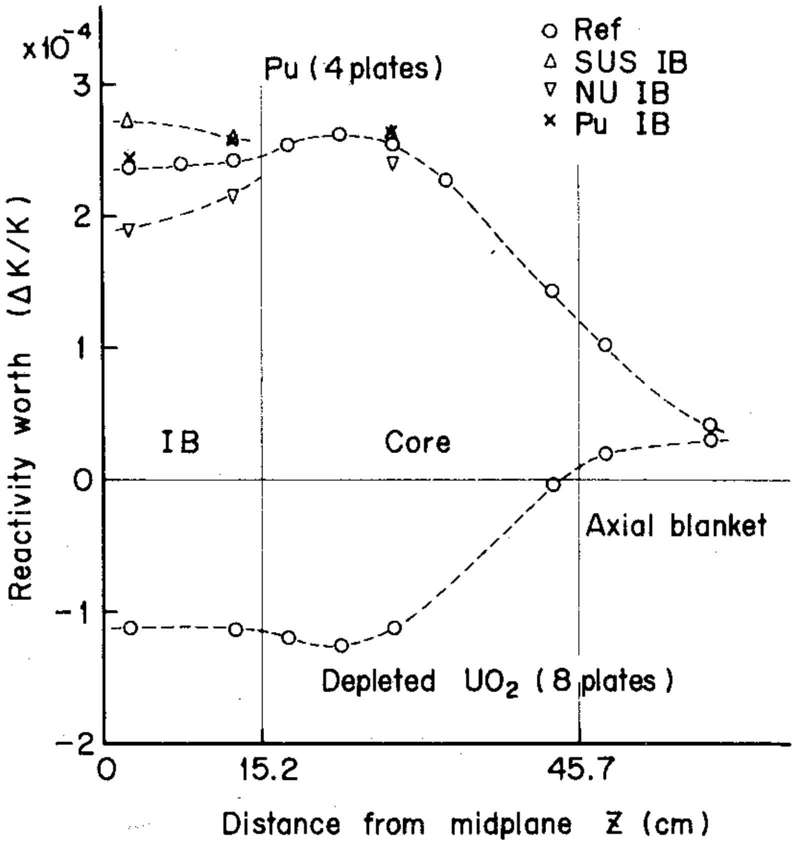


Fig. 6 Axial distributions of Pu and depleted $UO_2$ sample worths measured in FCA Assembly VII-3-1.

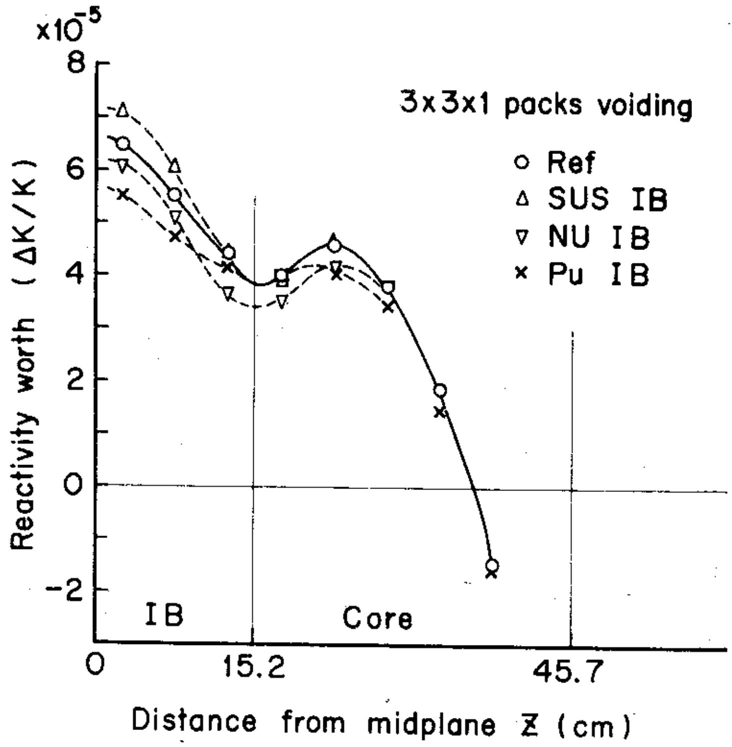


Fig. 7 Axial distributions of sodium void worth measured in FCA Assembly VII-3-1.

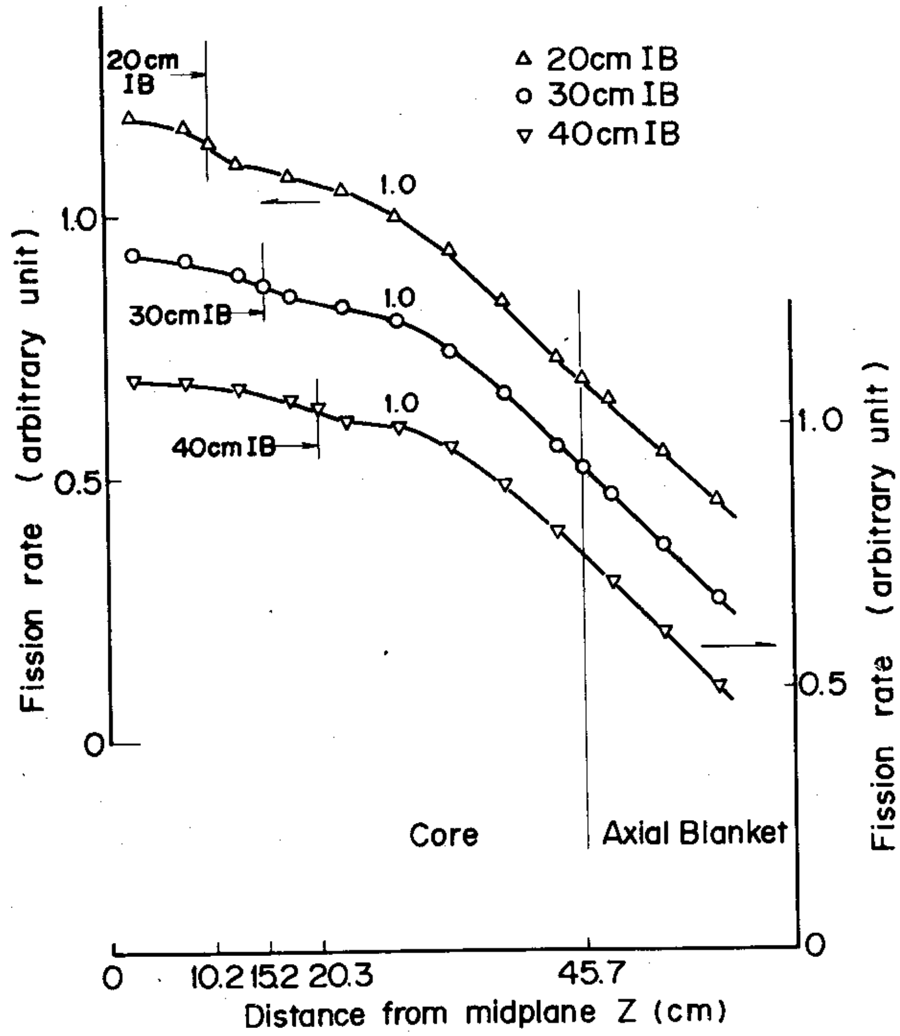


Fig. 8 Axial fission rate distributions of Pu-239 mfc measured in FCA Assembly VII-3.

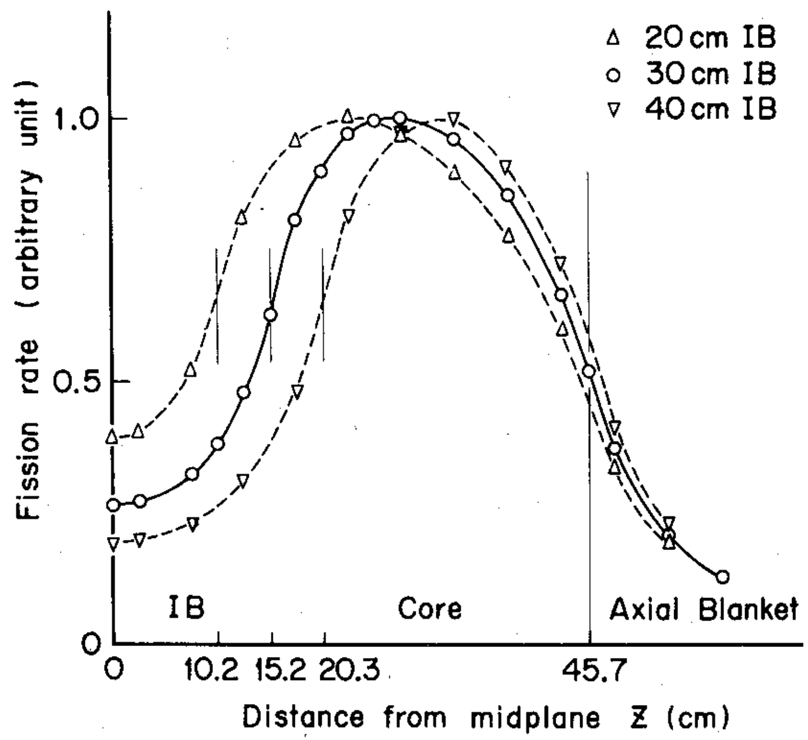


Fig. 9 Axial fission rate distributions of depleted U mfc measured in FCA Assembly VII-3.

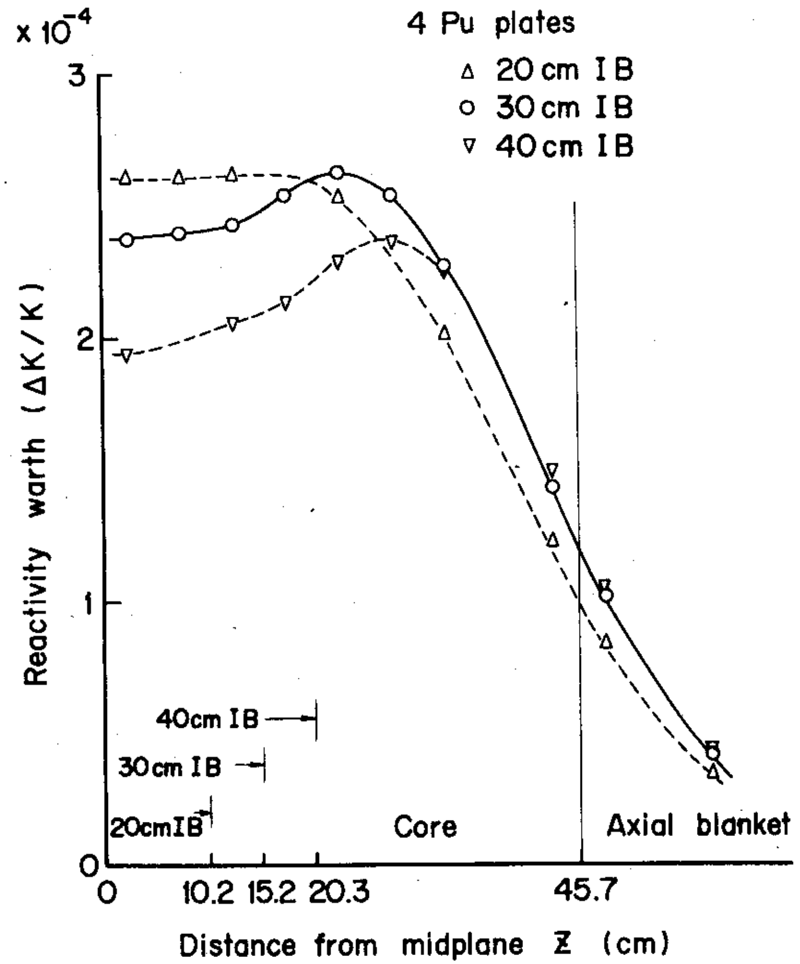


Fig. 10 Axial distributions of Pu sample worth measured in FCA Assembly VII-3.

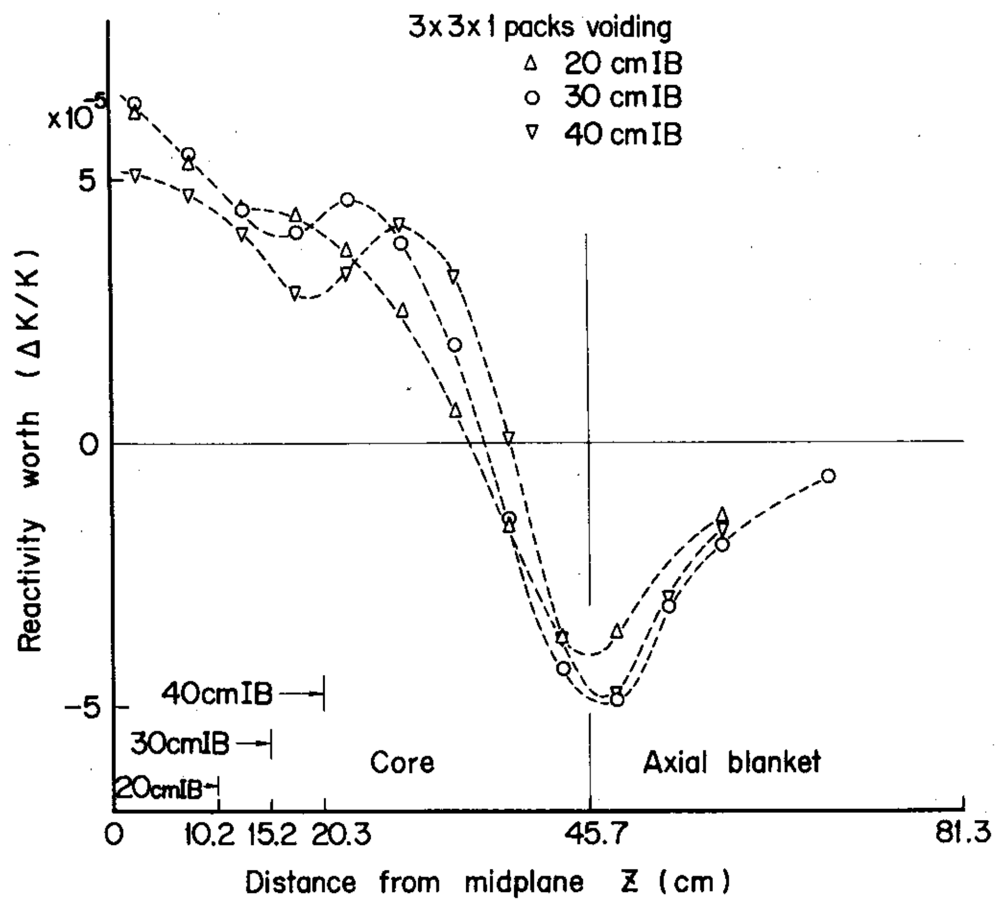


Fig. 11 Axial distributions of sodium void worth measured in FCA Assembly VII-3.

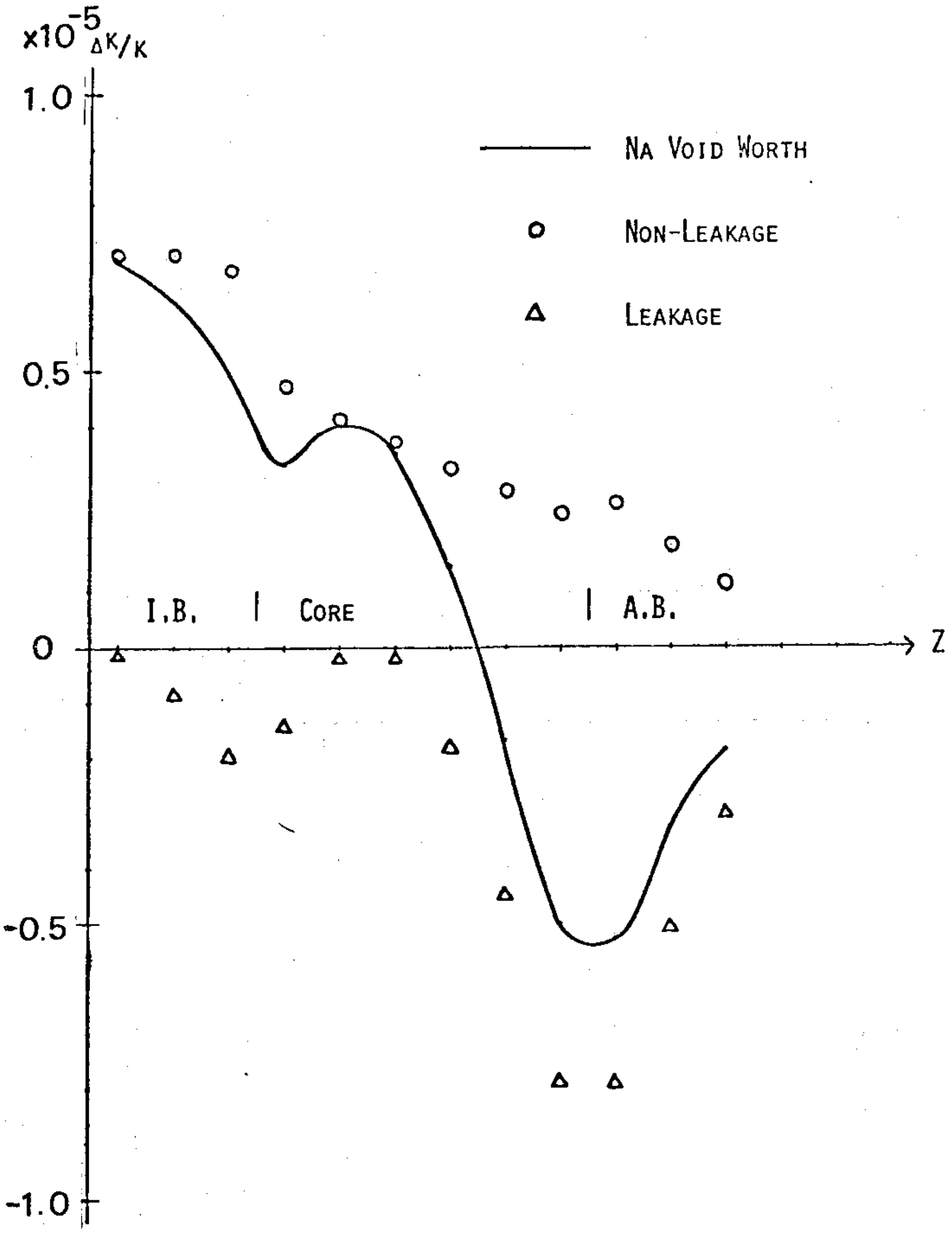


Fig. 12 Axial distribution of the calculated sodium void worth for FCA Assembly VII-3-1.